

Analysis of Fast and Slow Particles Production from the Interaction of ^{24}Mg with Emulsion Nuclei at 4.5A GeV/c

A. Abdelsalam, E. A. Shaat, Z. Abou-Moussa, B. M. Badawy⁽¹⁾, and Z. S. Mater
Physics Department, Faculty of Science, Cairo University, Egypt.

⁽¹⁾ *Reactor Physics Department, Nuclear Research Center, Atomic Energy Authority Egypt.*
E. Mail: he_cairo@yahoo.com

Received: 10/1/2012

Accepted: 16/2/2012

ABSTRACT

The target fragmentation of emulsion nuclei in the interaction of ^{24}Mg projectile at 4.5A GeV/c is investigated. The rapidity and angular distributions of the emitted fragments (grey and black) are analyzed in terms of the statistical model. The mean longitudinal velocities and the characteristics spectral velocities of the particle emitting system are determined. The temperatures T of the emitting system for grey and black particles (60 and 6 MeV respectively) are found to be independent of the projectile mass number and target size. The experimental range–energy distributions as well as the relationship between the energy and the rate of energy loss for both the grey and black particles can be described well by the outputs of a special computer program called SRIM. The kinetic energy distributions of produced grey and black particles are presented in power law relations and agree well with the predictions of the cascade evaporation model.

Keywords: ^{24}Mg Interactions with Emulsion / Angular and Rapidity Distributions / Energy–Range Relationship / Energy Distribution.

INTRODUCTION

Most of the experimental work dealing with high energy nucleon-nucleus and nucleus-nucleus interactions is concerned with the study of the characteristics of the emitted secondary particles. The use of heavy nuclei as targets in relativistic particle collisions enables scientists to study the effective parameters and mechanisms responsible for the production of such secondaries. Using nuclear emulsion as both target and detector is very suitable for the required studies because it records all charged secondary particles of an individual event in 4 π -geometry due to high spatial resolution.

In this paper, the interaction of 4.5 A GeV/c ^{24}Mg with different emulsion nuclei has been studied. The angular distribution, the rapidity, the energy- range relationship and the energy distribution for grey and black particles are presented and explained in terms of the statistical evaporation model⁽¹⁾.

EXPERIMENTAL DETAILS

This work is carried out using a nuclear emulsion stack of type NIK-FI-BR-2 where the dimensions of each pellicle are 10 cm \times 20 cm \times 60 μm .

This stack was exposed to a 4.5 A GeV/c ^{24}Mg ion beam from JINR Synchrophasotron at Dubna – Russian. The stack has a sensitivity of about 30 grains per 100 μm for singly charged minimum ionizing particles. Only very thick dark beam tracks, a part from the surface and bottom by at least 20 μm were chosen for along the track double scanning, fast in the forward direction and slowly in the backward one.

Since, through a total scanned length of 103.06 meters of beam tracks, 1094 inelastic interactions with emulsion nuclei were detected, the experimental mean free path " λ_{exp} " = 10.15 ± 0.29 cm.

The secondary tracks emerging from each interaction are classified according to the emulsion terminology depending on their appearance under the microscope. These tracks are either shower (N_s) or grey (N_g) or black (N_b) ones. The shower tracks ($\beta > 0.7$) correspond to singly charged relativistic particles (mainly pions with kinetic energy < 60 MeV), where the grey ($0.3 < \beta < 0.7$) and black ($\beta < 0.3$) tracks are produced by comparatively slower fragments emitted from the target nucleus. Grey tracks are mostly recoil protons with kinetic energy $26 < \text{K.E} < 400$ MeV while black tracks are due to protons of kinetic energy < 26 MeV. The grey and black tracks are denoted as tracks of heavily ionizing particles N_h (i.e. $N_h = N_g + N_b$)

STATISTICAL MODEL

Considering the number of observed events large enough, it is possible to apply practically the statistical hypothesis of equal prior probabilities in phase space. This allows the use a modified Maxwellian distribution for the momentum (P) or velocity (β) of the emitted fragments (protons) of the form⁽¹⁾,

$$d^2 N / dP d\mu \propto P^2 \exp \left[- \left(P^2 - 2M\beta_{//} P \mu \right) / P_o^2 \right] \quad (1)$$

$$d^2 N / d\mathbf{b} d\mu \propto \mathbf{b}^2 \exp \left[- \left(\mathbf{b}^2 - 2\mathbf{b}_{//} \mu \right) / \mathbf{b}_o^2 \right] \quad (2)$$

where, $\beta_{//}$ is the longitudinal velocity component of the particle emitting system, $\mu = \cos(\theta)$, where θ is the laboratory angle between the momentum of the fragment of mass M and the momentum of the initial projectile and $P_o = M\beta_o = (2ME_o)^{1/2}$ where E_o is the characteristic energy per particle in the hypothetical moving system. Following the assumptions mentioned below:

- The observed range and angle distributions are interpretable in terms of a single Maxwellian range (velocity) distribution.
- The isotropic distribution of the fragments is dominated by protons, thereby minimizing any significant difficulties in defining \mathbf{b}_o in the Maxwellian distributions (1).
- The $\mathbf{b}_{//}$ and \mathbf{b}_o parameters which characterizing the range and angular distributions are thus the same as those describing the velocity distribution for protons. The coulomb barrier effects are negligibly small.

With these assumptions, the probability distribution for the longitudinal velocity component of the fragment (proton) β_L , where $\mathbf{b}^2 = \mathbf{b}_L^2 + \mathbf{b}_T^2$, reduces to Gaussian form,

$$dN / dy \approx e^{- (y - y_o)^2 / 2s^2} \quad (3)$$

The rapidity variable y is related to β_L via $\beta_L = \tanh(y) \sim y$ ($\beta_L < 1$), where $y = \beta_L = \beta_{//}$ is the first moment and, $s^2(y) = s^2(\beta) = (\beta_o^2/2) = (E_o/M)$ is the variance of the β_L distribution. This variance can also be expressed in the form; $s^2(T) = (T/M_n)$, where T is the equivalent temperature of the system and M_n is the nucleon rest mass.

Integrating equation (2) over β for the first order of $(\beta_{//}/\beta_o)$, one can get the following angular distribution of the emitted particles:

$$dN / d\mathbf{m} \approx (C [b_o / 4] \sqrt{p}) (F / B)^m \quad (4)$$

or

$$dN / dq \propto \sin q (F / B)^{\cos q} \quad (5)$$

where F/B is the ratio of the number of fragments in the forward hemisphere to that in the backward one, and the anisotropy ratio (F/B) can be expressed as:

$$(F / B) \approx \exp\left[(4/\sqrt{p}) b_{//} / b_o\right] \quad (6)$$

RESULTS AND DISCUSSION

Angular Characteristics of Grey and Black Particles

In this section, we focus our attention on the characteristics of the grey and black target fragments. These fragments are produced by tracks with energy ranges $26 < E_g < 400$ MeV and $E_b < 26$ MeV respectively. Table (1) represents the mean angles of the emitted grey and black particles $\langle \theta \rangle_g$ and $\langle \theta \rangle_b$ in $^{24}\text{Mg} - \text{Em}$ interaction with the corresponding values for different projectiles⁽²⁻⁵⁾. One can notice that, the values of the mean angles $\langle \theta \rangle_g$ and $\langle \theta \rangle_b$ are nearly independent of the projectile mass number. In figure (1) and (2) the angular distributions for grey and black particles emitted in the present interaction are shown. From these figures, it can be seen that:

- The distributions show a peaking shape with peak positioned nearly at $\theta = \langle \theta \rangle_g$ and $\theta = \langle \theta \rangle_b$.
- The number of the backward emitted particles (i.e. with $\theta > 90^\circ$) decreases with increasing θ .
- The distributions of such backward angles follow an exponential decay.
- The angular distributions of grey and black particles can be reproduced successfully using the statistical model prediction i.e. equation (5). These predictions are presented in figures (1) and (2) by smooth curve.

Table (1): The mean angle of emission of grey and black particles at incident momentum of 4.5A GeV/c.

Projectile	$\langle \theta \rangle_g$	$\langle \theta \rangle_b$	Ref.
p	67.80±1.20	85.30±1.90	(2)
^4He	62.8±3.10	83.00±3.3.80	(2)
^6Li	64.90±2.2	82.20±2.60	(3)
^7Li	63.50±2.00	81.30±2.30	(4)
^{12}C	64.00±1.90	79.50±2.10	(2)
^{22}Ne	63.70	—	(5)
^{24}Mg	56.50±4.50	85.72±4.72	Present Work
^{28}Si	63.30	—	(5)

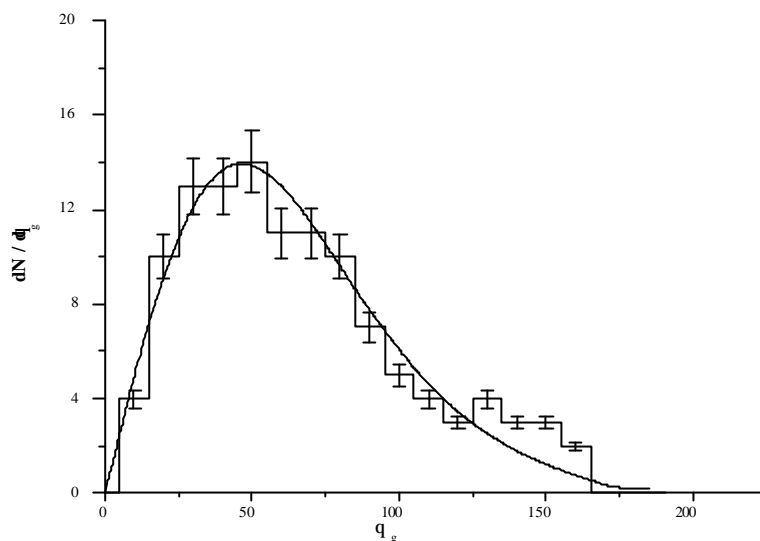


Fig. (1): The angular distribution of the grey particles emitted in the interaction of ^{24}Mg with emulsion, together with the prediction of statistical model (smooth curve).

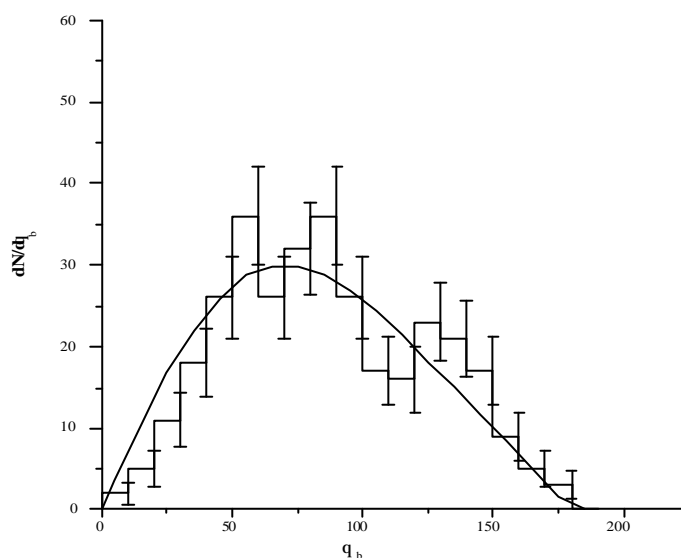


Fig. (2): The angular distribution of the black particles emitted in the interaction of ^{24}Mg with emulsion, together with prediction of statistical model (smooth curve).

Rapidity Distributions of Grey and Black Particles

One of the important processes of the complex mechanism of the nucleon - nucleus and nucleus - nucleus interaction is the fragmentation of the target nuclei due to the inelastic interaction with relativistic projectile nuclei. A lot of information concerning the dynamics of the fragmentation processes is given by the studying of the rapidity distribution of the target fragments. Therefore, this section deals with analyzing the rapidity distribution characteristic of grey and black particles emitted in the present ^{24}Mg -Em interaction.

In figure (3) and (4), the present rapidity distributions of grey and black particles are shown by a histogram. The corresponding fitting, for each, by the well known Gaussian shape is illustrated by the

smooth curve. The present data are then divided into two groups of events according to the accompanied N_h values (i.e. $N_h < 7$ and $N_h > 7$). The corresponding rapidity distributions for grey and black particles, together with their Gaussian fitting are drawn in Figs (5), (6), (7) and (8) respectively.

The main items characterizing the distributions in Figs (5), (6), (7) and (8) are:

- The peaking shape, where the peak occurs in the forward rapidity region.
- The well fitting by Gaussian shapes.
- The ranging of rapidity values for grey and black particles nearly between - 0.80 and +0.80 and -0.20 and +0.20, respectively.

For the rapidity distributions of grey particles, the Gaussian peak is positioned at $y_g = 0.205 \pm 0.026$ in Fig. (3), while in Fig. (5 and 7) it is positioned at $y_g = 0.244 \pm 0.026$ and 0.198 ± 0.039 , respectively. Since the target fragmentation regions of $N_h < 7$ and $N_h > 7$ represent the light and heavy target regions, respectively, then it can be said that for light target the shift of the distribution peak from the zero rapidity point is more than that for heavy target. In addition, one can observe that the distribution tends to be more symmetric around the peak position for higher target size. According to the statistical model, the peak position may represent the longitudinal velocity of the particle emitting system ($y = \beta_L$), therefore, the higher is the target size, the lower is the longitudinal velocity.

In the Figs (4) , (6) and (8), the positions of the Gaussian peaks are nearly at the same point with respect to zero rapidity point irrespective of the target size. So that, the target fragmentation seems to be completely limited and saturated for the black particle emitting system.

Characteristic Parameters of the Grey and Black Particles Emitting System

Now, in the light of the statistical model, the grey and black particles emitting systems can be distinguished by main parameters, such as, the longitudinal velocity ($\beta_{//}$), spectral velocity (β_o) and temperature T. The rational value of the velocity $\beta_o = \beta_{//} / \beta_o$ can be compared with experimental ones by substituting the experimental values of (F/B) in equation (6).

Table (2) and (3) show the values of $\beta_{//}$, s and T for both the present data and the corresponding ones for different projectiles at the same momentum per nucleon. The velocity β_o of the emitting system and the experimental values of the rational velocity β_o are also listed in these tables. From the present tables, one can see that:

- The mean longitudinal velocity $\beta_{//}$ of the grey particle emitting system for each projectile seems to depend on the target size such that it slightly decreases with increasing N_h . This may be due to the increase of cascading (secondary) collisions in the heavier target. On the other hand, the $\beta_{//}$ of the black particle emitting systems are small where they are ranging from 0.01 to 0.02 irrespective of projectile, energy and target.

- The half width s for all the grey rapidity distributions is the same within experimental errors. In other words, it is independent of the target size and projectile mass number. This may be due to the fixed energy range for these particles ($26 < E_g < 400$ MeV), which results in the same angular spread (but not multiplicity) for all groups of interactions⁽⁸⁻¹⁰⁾. Similar observation can be obtained for all the black rapidity distributions. The same result, as should be, is also true for the characteristic velocity β_o of each of the two emitting system.

- The temperature of the emitting system of grey particles can also be considered to be independent of the projectile mass number and target size, since its value is found to be around 60 MeV.

- The present temperature T , of the emitting system of the black particles for different target sizes has values in the range $T \sim 4.86$ to 5.71 MeV. Such temperature range is of the same order of magnitude of the binding energy/nucleon in nuclei and is also compatible with the temperature associated with the projectile fragmentation^(1, 12). This result confirms the limiting fragmentation hypothesis^(13, 14), and its onset at such incident energy/nucleon.

- The ratio (F/B) for each of the grey and black particles seems to be independent of the incident energy in the energy range at which the comparison is carried out (2.2 – 3.7A GeV).

- For each of the grey and black particles, the velocity ratio $(\beta_{//} / \beta_o)$ as calculated from the experimental ratio of (F/B) , agrees satisfactorily with the value obtained from the rapidity distribution. This means that the mean velocity $\beta_{//}$ of the grey and black particles emitting system can be calculated directly just from the ratio (F/B) (knowing that β_o is constant).

- Finally, the main conclusion is that, the grey and black particles may be emitted as a result of thermalization system, at its first and second stages.

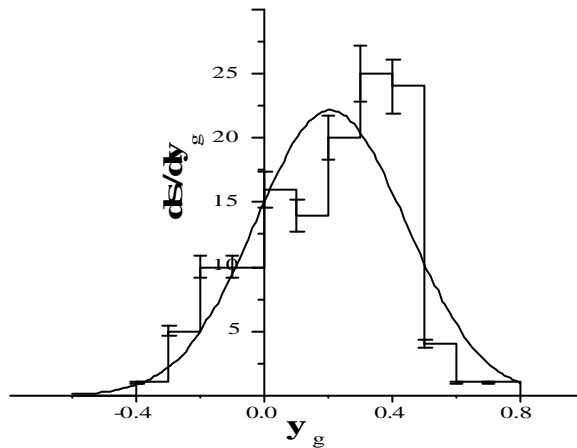


Fig. (3): The rapidity distribution for grey particles emitted in $^{24}\text{Mg-Em}$ interaction at $4.5A$ GeV/c.

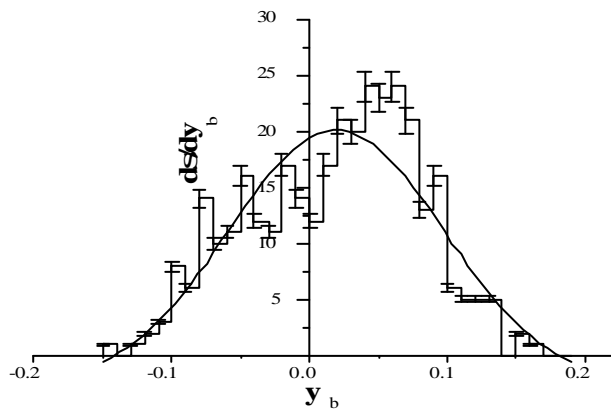


Fig. (4): The rapidity distribution for black particles emitted in $^{24}\text{Mg-Em}$ interaction at $4.5A$ GeV/c.

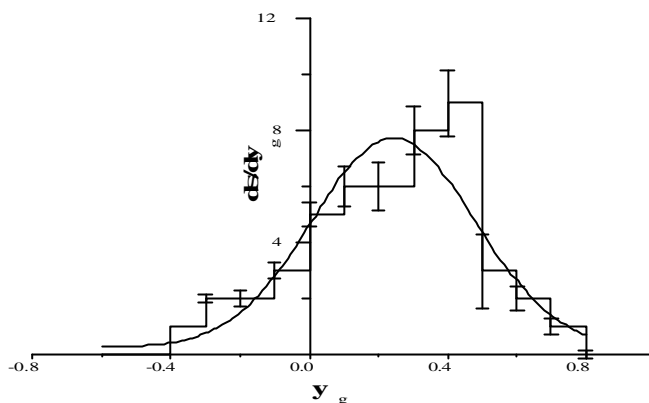


Fig. (5): The rapidity distribution for grey particles emitted in 4.5A GeV/c ^{24}Mg -Em interaction at $N_h \approx 7$.

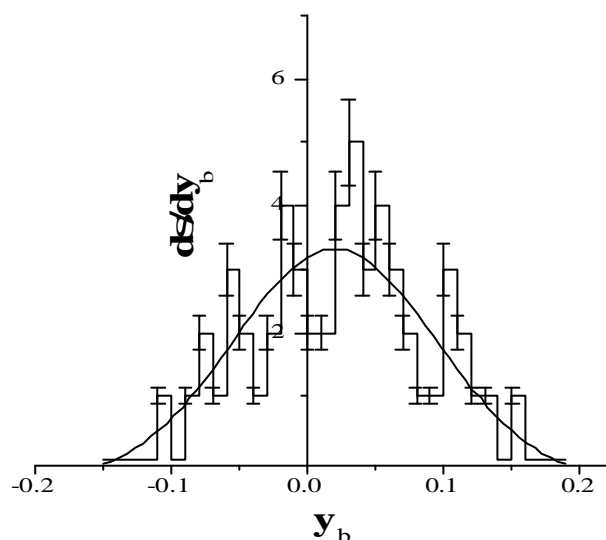


Fig. (6): The rapidity distribution for black particles emitted in 4.5A GeV/c ^{24}Mg -Em interactions at $N_h \approx 7$.

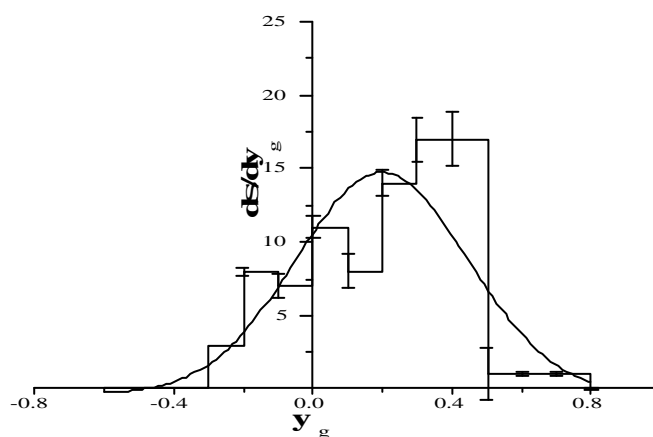


Fig. (7): The rapidity distribution for grey particles emitted in 4.5A GeV/c ^{24}Mg -Em interaction at $N_h > 7$.

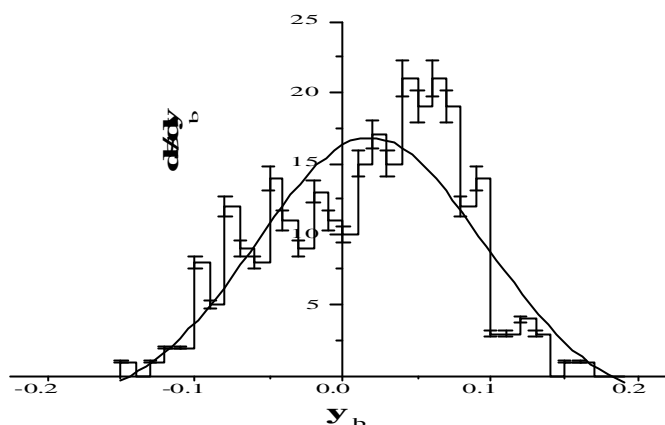


Fig. (8): The rapidity distribution for black particles emitted in 4.5A GeV/c ²⁴Mg–Em interaction at N_h > 7.

Table (2): Characteristics parameter of the grey particles emitting system for different interactions.

Projectile	Incident Energy	N _h	β _{//}	s(y)	β ₀	F/B	T MeV	τ ₀
p	3.7	< 7	0.186±0.014	0.264±0.013	0.373±0.013	3.010±0.100	65.300	0.510
		7-28	0.157±0.018	0.250±0.008	0.352±0.012	2.960±0.140	58.100	(0.490) 0.460 (0.480)
p	3.7	Total Sample				3.800±0.200		
⁴ He	3.7	< 7	0.234±0.013	0.245±0.010	0.346±0.020	4.290±0.130	58.700	0.680
		7-28	0.186±0.016	0.251±0.010	0.354±0.010	2.920±0.080	56.100	(0.640) 0.530 (0.480)
		> 28	0.141±0.020	0.251±0.013	0.354±0.020	2.710±0.240	58.800	0.480 (0.440)
⁴ He	3.7	Total Sample				3.000±0.300		
⁶ Li	3.7		0.110		0.350	2.900±0.200 2.15±0.140	57.500	
⁷ Li	2.2		0.190		0.350	3.820 2.780±0.200		
¹² C	3.7	< 7				4.210±0.150		(0.640)
		> 0				3.550±0.190		(0.560)
		> 14				3.370±0.180		(0.540)
¹² C	3.7	Total Sample				3.510±0.200		
¹⁴ N	2.1					3.690		
²² Ne	3.3					3.500±0.120		
²⁴ Mg	3.7	< 7	0.244±0.026	0.236±0.036	0.334±0.051	4.950±0.130	52.240	0.715
		> 7	0.198±0.039	0.247±0.056	0.349±0.079	3.597±0.170	57.230	(0.704) 0.567 (0.567)
		Total Sample	0.205±0.026	0.236±0.046	0.334±0.065	3.847±0.150	52.024	0.597 (0.597)
²⁸ Si	3.7	Total Sample				3.520±0.160		

Table (3): Characteristic parameters of the black particles emitting system for different interactions.

Projectile	Incident Energy	N_h	$\beta_{//}$	$s(y)$	β_o	F/B	T M eV	β_o	Ref.
P	3.7	< 7 7- 28	0.010±0.001 0.010±0.002	0.069±0.002 0.078±0.061	0.097±0.010 0.110±0.012	1.290±0.090 1.270±0.070	4.560 5.700	0.102 (0.113) 0.091 (0.106)	(6)
P	3.7	Total Sample				1.280±0.100			(2)
⁴ He	3.7	< 7 7- 28 > 28	0.016±0.003 0.016±0.004 0.015±0.003	0.071±0.002 0.077±0.002 0.077±0.003	0.100±0.019 0.109±0.006 0.100±0.010	1.540±0.080 1.370±0.080 1.380±0.120	4.700 5.600 5.700	0.168 (0.190) 0.100 (0.139) 0.150 (0.143)	(6)
⁴ He	3.7	Total Sample				1.350±0.100			(2)
⁶ Li	3.7	Total Sample	0.012		0.115	1.290±0.060			(7)
⁷ Li	2.2	Total Sample	0.020		0.115	1.480±0.700	6.8		(7)
¹² C	3.7	< 7 > 0 > 14						(0.110) (0.106) (0.095)	(6)
¹² C		Total Sample				1.270±0.100			(2)
⁴ He*	2.1	Total Sample	0.016±0.004	0.083	0.117±0.002	1.770±0.080	6.400		(1)
¹⁶ O*	2.1	Total Sample	0.015±0.002	0.083±0.014	0.115±0.002	1.240±0.080	6.200		(1)
⁴⁰ Ar*	2.1	Total Sample	0.012±0.002	0.083±0.002	0.117±0.002		6.400		(1)
²⁴ Mg	3.7	< 7 > 7	0.020±0.003 0.018±0.005	0.074±0.014 0.077±0.015	0.102±0.002 0.110±0.002	1.556±0.030 1.447±0.046	4.860 5.56	0.196 (0.196) 0.164 (0.164)	Present Work
						1.477±0.054	5.710	0.173 (0.172)	

*The experimental values of the rational velocity β_o are placed in this table between parentheses

Range – Energy relationship

In this work, the range – energy relationship was obtained for each detected grey particle emitted from the 4.5A GeV/c ²⁴Mg - emulsion interaction. This was carried out by measuring the length of each grey particle's trajectory and evaluating its deviation due to coulomb scattering following the coordinate method. Then, the corresponding kinetic energy was calculated. On the other hand, for the black particles emitted from present interaction the kinetic energy of each particle was calculated according to the value of its range using the range – energy equation [$R = (E_p / 9.3)^{1.8}$ in Ref (15)].

The present range-energy distributions of the grey and black particles are shown in figure (9) and (10), respectively together with the corresponding distributions calculated by using SRIM program⁽¹⁵⁾. This program is a collection of software packages which calculates both the stopping power of medium through which an incident ion passing (with energy from 10 KeV up to 4 GeV) and the range traversed by this ion. From these figures, one can notice, the good agreement between the experimental distribution and the outputs of the used computer program.

The experimental and SRIM data are approximated by the following simple dependence,

$$R = a E^b \quad (7)$$

Such approximations are displayed on figure (9) and (10) by the smooth curves. Table (4) represents the fitting parameters of the experimental and SRIM data "a_g", "β_g", "a_b" and "β_b". One can observe from Table (4) that the fitting parameters of the experimental data are in a good agreement with those of the SRIM calculations.

Table (4): The values of the experimental and SRIM fitting parameters a_{g,b} and β_{g,b} for the grey and black range - energy distributions.

Particles		Fitting Parameters	
		a _{g,b}	β _{g,b}
Grey	Present Work	0.0124±0.0005	1.7000±0.0045
	SRIM Program	0.0117±0.0005	1.7010±0.0045
Black	Present Work	1.6900±0.0025	12.6730±0.0978
	SRIM Program	1.7100±0.0024	13.5000±0.0093

For each of the emitted grey and black particles, the rate of energy loss as a function of the energy was calculated and plotted in figure (11) and (12), respectively. The corresponding SRIM estimations are also drawn in these figures showing a good agreement with the present data. The experimental and SRIM results for grey and black particles are found to be fitted by the following exponential form:

$$\frac{dE}{dR} = A_1 e^{-E_b I_1} + A_2 e^{-E_b I_2} \quad (8)$$

The values of the experimental and SRIM fitting parameters A₁, β₁, A₂ and β₂ for these particles are shown in Table (5). This table reveals the good agreement between the parameters fitting the experimental and SRIM data.

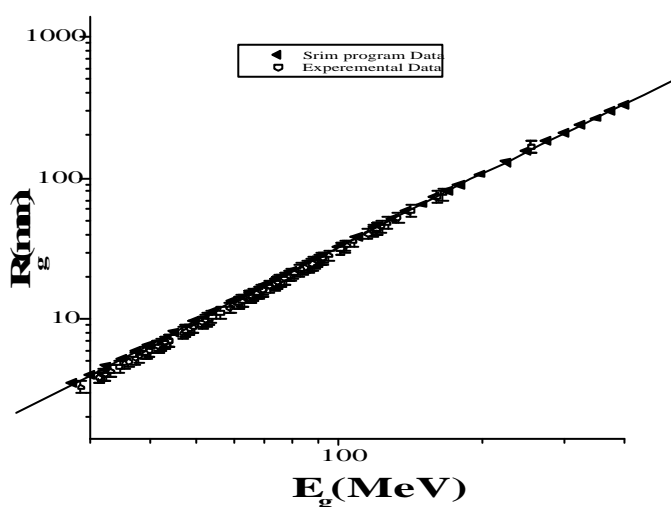


Fig. (9): The experimental distribution of the range – energy relation of the grey particles emitted in ²⁴Mg-Em interactions compared with the corresponding theoretical one.

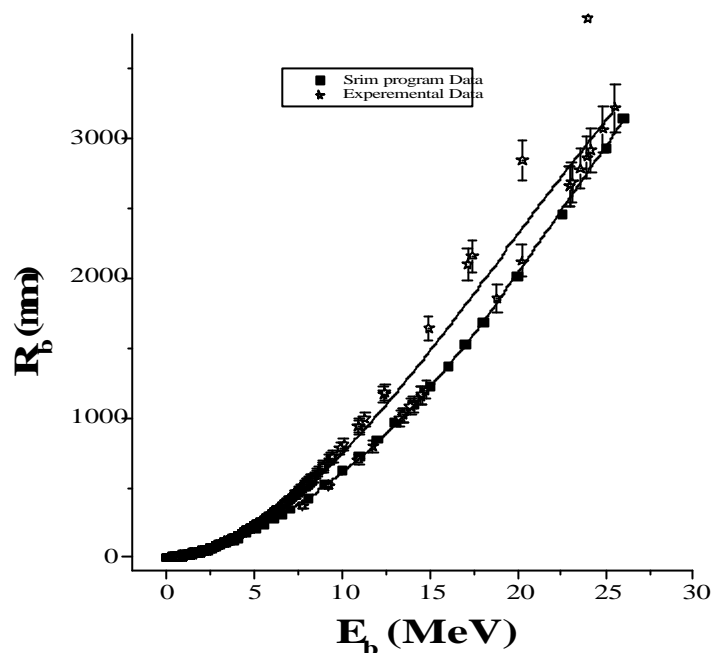


Fig. (10): The experimental distribution of the range-energy of the black particles emitted in $^{24}\text{Mg-Em}$ interactions compared with the corresponding theoretical one.

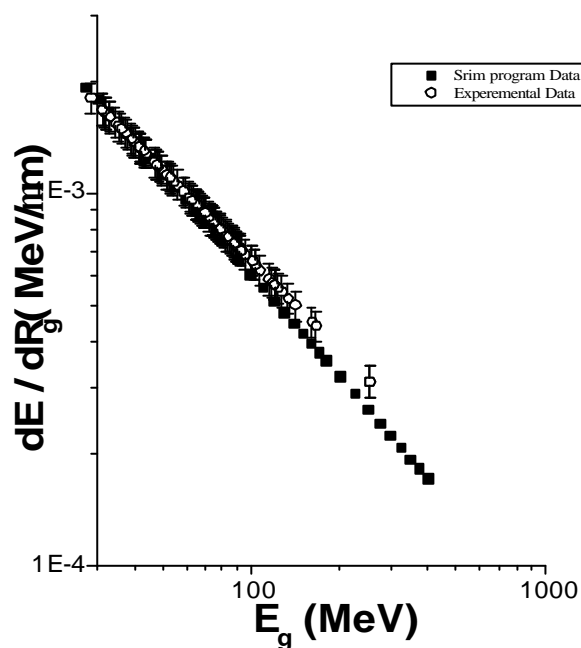


Fig. (11): The distributions of rate of energy lose of the grey particles emitted in $^{24}\text{Mg-Em}$ interaction compared with the corresponding theoretical one.

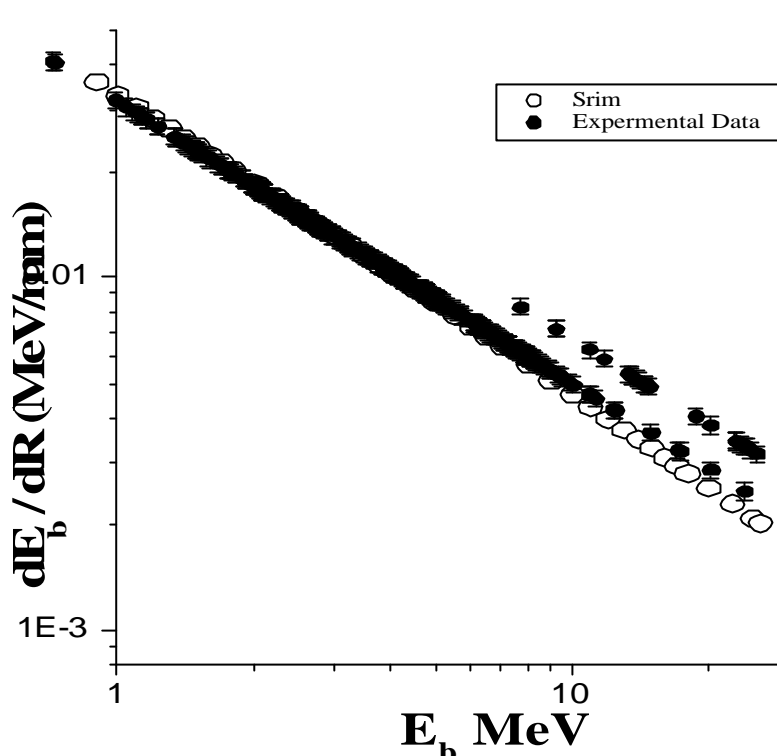


Fig. (12): The distribution of rate of energy loss of the black particles emitted in ²⁴Mg–Em interaction compared with the corresponding theoretical one.

Table (5): The values of the experimental and SRIM fitting parameters for the grey and black distributions of figures (11, 12).

Fitting Parameters	Grey Particles	Black Particles
A ₁	0.0033 ± 0.0003* 0.0039 ± 0.0010	0.0779 ± 0.0015* 0.0740 ± 0.0013
? ₁	0.0604 ± 0.0060* 0.0549 ± 0.0020	1.9262 ± 0.0366* 1.6921 ± 0.0490
A ₂	0.0014 ± 0.0001* 0.0012 ± 0.0004	0.02311 ± 0.0004* 0.02017 ± 0.0003
? ₂	0.0122 ± 0.0002* 0.0121 ± 0.0003	0.3125 ± 0.0060* 0.2508 ± 0.0040

These fitting parameters are calculated using SRIM program.

Finally, the kinetic energy distributions of both the present grey and black particles were obtained. Figures (13) and (14), represent such distributions together with the corresponding predictions of the cascade-evaporation model (CEM) (the histograms). The experimental data are approximated by the following simple dependence,

$$\frac{dN}{dE} \approx E^{-a} \quad (9)$$

Such approximations are display on the figures by the smooth curves, where the fitting parameters of the experimental data "a_g" and "a_b" can be found to be 1.40 ± 0.10 and 1.55 ± 0.20,

respectively. These values are found to match those obtained by the authors of ref (16). It can be seen from figures (13) and (14) that the experimental data can be described well by the distribution calculated following the (CEM).

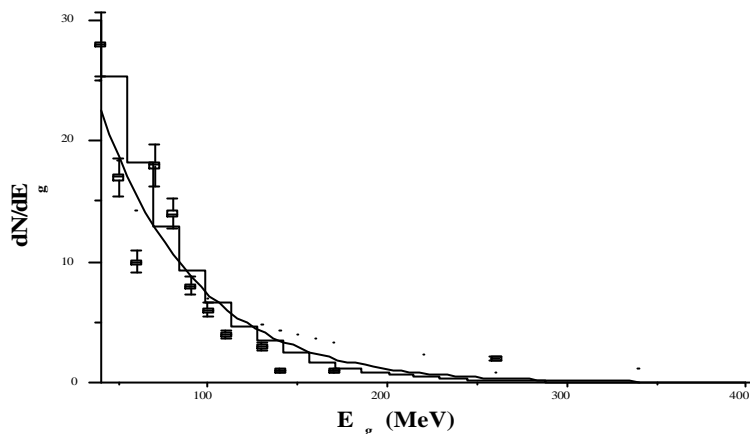


Fig. (13): The energy distribution of grey particles emitted in the interactions of 4.5A GeV/c ^{24}Mg with emulsion nuclei. The histogram represents the corresponding theoretical energy distribution calculated according to CEM model. The smooth curve represents the approximated fitting of the data.

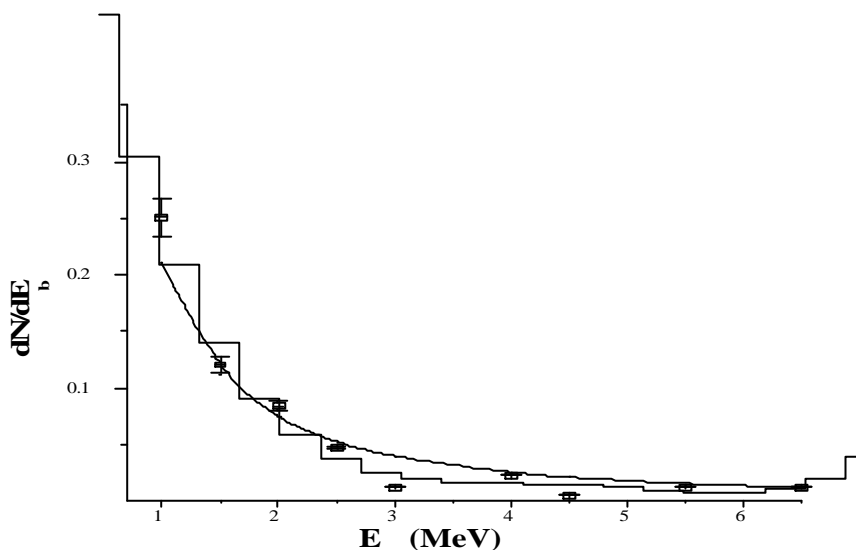


Fig. (14): The energy distribution of black particles emitted in the interactions of 4.5A GeV/c ^{24}Mg with emulsion nuclei. The histogram represents the corresponding theoretical energy distribution calculated according to CEM model. The smooth curve represents the approximated fitting of the data.

For the sake of comparison, the present energy distribution of the grey particles is represented in figure (15) together with the corresponding distributions obtained for interactions with nuclear emulsion of 4.5 GeV/c $p^{(17)}$ and 4.1A GeV/c $^{22}\text{Ne}^{(18)}$. These three distributions can be fitted by the following exponential form:

$$\frac{dN}{dE_g} = A e^{-E_g / \tau_g} \quad (10)$$

The values of the fitting parameters "A" and τ_g (where τ_g is the decay constant) for the three compared interactions are displayed in the Table (6). It can be noticed from the figure that, the three represented distributions follow the same trend. However, one can see that the grey particle kinetic energy " E_g " in the case of ^{24}Mg and ^{22}Ne projectiles are extended to higher range and have more probable values than those for the p projectile . This is due to the fact that the increase of the mass number of the incident projectile and hence the increase of the number of colliding nucleons, the more the number of the emitted recoil and cascading protons.

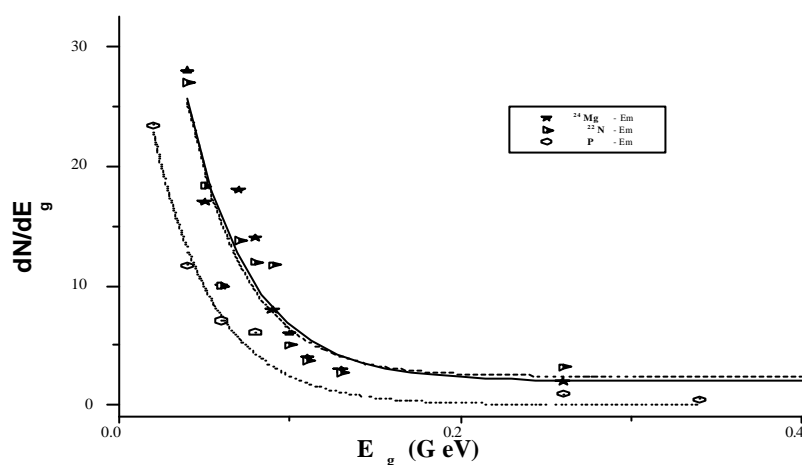


Fig. (15): Energy distribution of grey particles emitted in the interactions of 4.5A GeV/c p⁽⁷⁵⁾, 4.1A GeV/c, ²²Ne⁽⁷⁶⁾, and 4.5A GeV/c ²⁴Mg with emulsion nuclei. The smooth curves represent the corresponding energy distributions which are calculated according to the experimental decay fitting.

From the study of the particles emitted in the interaction of 4.5A GeV/c ²⁴Mg with emulsion nuclei, the following conclusions can be drawn:

Table (6): The values of the experimental fitting Parameters A and τ_g for the grey distributions of figure (15).

Projectile	Fitting Parameters		Ref.
	A	τ_g	
4.5 GeV/c p	39.91 ± 4.13	27.78	(34)
4.1A GeV/c ²² Ne	74.29 ± 24.79	29.91	(35)
4.5A GeV/c ²⁴ Mg	69.01 ± 21.31	27.03	Present Work

CONCLUSION

- 1) The average emission angles of the grey and black particles $\langle \theta \rangle_g$ and $\langle \theta \rangle_b$ are nearly independent of the projectile mass number.
- 2) The experimental angular distributions for grey and black particles agree with the empirical one obtained using a Gaussian form equation.
- 3) The mean longitudinal velocity ($\beta_{//} = v$) of the grey particles emitting system seems to depend on the target size such that it decreases with increasing N_t . This could be attributed to the increase of cascading (secondary) collisions in the heavier target. For the black particles, $\beta_{//}$ are small where $0.01 < \beta_{//} < 0.02$ irrespective of the incident energy or projectile.
- 4) The temperature of the grey particles emitting system can also be considered to be independent of the projectile mass number and target size, since its value is found to be around 60 MeV.
- 5) The present temperature T , of the emitting system of the black for different target sizes has values which are nearly ranging from 4.86 up to 5.71 (MeV). This temperature is of the same order of magnitude of the binding energy per nucleon in nuclei and is also compatible with the temperature associated with the projectile fragmentation. This result confirms the limiting fragmentation hypothesis and its onset at such incident energy/nucleon.
- 6) The experimental range - energy distributions for grey and black particles can be described by the outputs of the used SRIM program.
- 7) The present experimental data concerning the rate of energy loss as a function of the energy for the emitted grey and black particle are in a good agreement with those calculated according to SRIM program.
- 8) The present experimental kinetic energy distributions of both the grey and black particles can be described well by the distributions calculated following the CEM.
- 9) The comparison between the present grey kinetic energy distribution and the corresponding ones obtained for other projectiles at the same incident momentum per nucleon indicates that as the increase of the number of the interacting nucleons, the more the number of the emitted recoil protons.

ACKNOWLEDGEMENT

This work was carried out at Mohamed El-Nadi High Energy Physics Laboratory, Physics Department, Faculty of Science, Cairo University, Egypt.

The authors would like to thank all the staff of (Vekseler and Baldin) High Energy Laboratory at JINR, Dubna, Russia, for providing us the irradiated emulsion plates.

REFERENCES

- (1) H. H. Heckman, H. J. Crawford, D. E. Greiner, P. L. Lindstrom, and Wilson Lamce; Phys. Rev. C ;17, 1651 (1978).
- (2) A. Abdelsalam; Phys. Scr.; 47, 124 (1993).
- (3) M.I.Adamovich; LUND Report LUIP; 8906 (1989).
- (4) M. El-Nadi; Il Nuovo Cimento A.; 107, 1 (1994).
- (5) M. M. Sherif; Il Nuovo Cimento A.; 109, 1135 (1996).
- (6) A. Abdelsalam; Phys. Scr.; 47, 505 (1993).
- (7) B. M. Badawy Ph. D. Thesis Nuclear Physics; (2001).
- (8) K. D. Tolstove; "Dubna-Frankfurt Cooperation and Comments to the International Conference on Extreme States in Nuclear Systems" (1980).
- (9) O. E. Badawy; Z. Phys. A.; 279, 407 (1976).
- (10) H. H. Heckman; Phys. Rev. Lett.; 28, 926 (1972).
- (11) J. V. Geaga; Phys. Rev. Lett.; 45, 1933 (1981).
- (12) A. M. Baldin; Proceedings of International Conference on Extreme States in Nuclear System Presden (1980).
- (13) J. Benecke, T. T. Chov, C. N. Yang, and E. Yen; Phys. Rev.; 88, 2159 (1969).
- (14) H. H. Heckman; Phys. Rev. Lett.; 28,926 (1972).
- (15) [Http:// WWW.Srim.Org / Index. Htm](http://WWW.Srim.Org/Index.Htm).
- (16) V. S. Barashenkov; "International of High Energy Particles and Atomic Nuclei with Nuclei", Atomizdat, Moscow (1972).
- (17) V. A. Antonchik; Sov. J. Nucl. Phys.; 45, 790 (1987).
- (18) V. G. Bogdanov; Sov. J. Nucl. Phys.; 38, 909 (1987).